Phys. Status Solidi C **9**, No. 6, 1411–1414 (2012) / **DOI** 10.1002/pssc.201100657

physica status solidi c
www.pss-c.com
current topics in solid state physics

Quantum Hall effect in bilayer and trilayer graphene

C. Cobaleda[1], F. Rossella[2], S. Pezzini[1,2], E. Diez[*,1], V. Bellani[2], D. K. Maude[3], and P. Blake[4]

[1] Laboratorio de Bajas Temperaturas, Universidad de Salamanca, 37008 Salamanca, Spain
[2] Dipartimento di Fisica "A. Volta" and CNISM, Università degli studi di Pavia, 27100 Pavia, Italy
[3] Laboratoire National des Champs Magnétiques Intenses, CNRS-UJF-INSA-UPS, 38042 Grenoble, France
[4] Manchester Centre for Mesoscience & Nanotechnology, University of Manchester, Manchester M13 9PL, United Kingdom

Received 28 September 2011, revised 28 October 2011, accepted 28 October 2011
Published online 14 March 2012

Keywords graphene, quantum Hall effect

* Corresponding author: e-mail enrisa@usal.es

We have performed magneto-transport experiments in bilayer and trilayer graphene, at temperatures between 2 and 190 K and magnetic fields up to 22 T. Here we study the observation of the quantum Hall effect in bilayer and trilayer graphene. We have observed the quantum Hall plateaus at $\nu = 4, 8, 12, 16, 20$ in bilayer graphene and the quantum Hall plateaus $\nu = \pm 6$ and studied their temperature dependence. We have also studied the symmetry properties which are related with different contact configurations and describe the method used to study inhomogeneous samples

1 Introduction Graphene is a fascinating material that has been studied in several investigations due to its unique electronic properties, which are interesting to study because of the theoretical concepts involved and its potential applications [1–5]. The electronic properties of graphene caused by its electronic band structure leads to unusual solid state effects, such as the massless dirac fermions in two dimensional electron gas and the anomalous quantum Hall effect (QHE) [1–8].

The resulting series of the quantum Hall plateaus for monolayer graphene is $\nu = \pm 2, \pm 6, \pm 10, \pm 14, \ldots$, whereas it is $\nu = \pm 4, \pm 8, \pm 12, \pm 16, \ldots$ for bilayer graphene (see Fig. 3). Because of the experimental observation of these series for the QHE in graphene [6–8] the electronic properties of graphene and multilayer graphene has been extensively investigated. In particular, QHE in trilayer graphene (TLG) has also been investigated since its band structure depends on the interlayer stacking sequence [9–13].

Here we show the QHE in both bilayer and trilayer graphene. In particular, we show the presence of the $\nu = \pm 6$ integer quantum Hall plateau in trilayer graphene. Furthermore, we will show a non symmetry arising due to the presence of a density gradient which is enhanced upon the reversal of the magnetic field. This result has been previously observed in 2DEG [14] and more recently in graphene [15, 16].

2 Experimental methods The samples have been fabricated by means of mechanical exfoliation of natural graphite. They were placed on different thick Si wafers covered by a 300 nm thick SiO_2 layer.

Using optical microscopy and micro-Raman measurements we determined the number of layers present in the graphene flakes. We measured the Raman scattering spectrum of the TLG Hall bar at room temperature, using a micro-Raman set-up with laser light excitation at 1.96 eV with ~ 1 mW/µm^2 power density. Figure 1 shows the characteristic Raman scattering "2D" band of the sample under study. Lui and co-workers [17] recently shown that the peculiar shape of the 2D Raman band provides a powerful tool for the analysis of the stacking in TLG. The Raman spectrum of our trilayer graphene device reported in Fig. 1 exhibits the multi-component feature characteristic of TLG, and according to Ref. [17] suggests the presence of a Bernal-stacking ABA. The inset of Fig. 1 depicts an

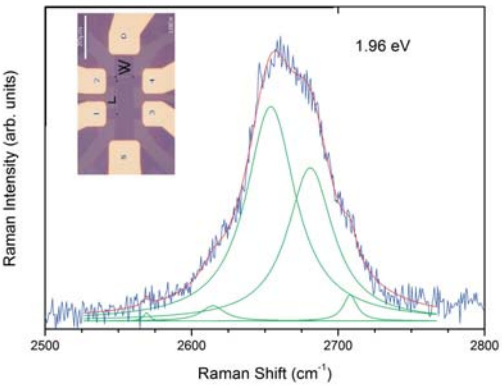

Figure 1 Raman spectrum of the TLG device used in this work. The inset shows a scheme of the two Hall bars used and the contacts labeled.

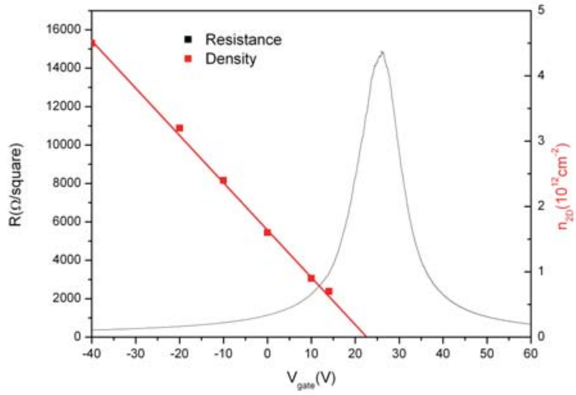

Figure 2 Longitudinal resistance measured at magnetic field $B = 0$ T using the gate voltage as driving parameter. The Dirac point was found at $V_G = 25$ V. The carrier density in the hole-like regime is shown in red.

optical image of the flake exfoliated and the Hall bar to be processed. The process procedure is done as follows: the Hall bar geometry was defined by means of photolithography (LaserWriter, 405 nm wavelength) with a “lift-off” process, and a bilayer stack of PMGI and S1805 was used for the resist. The contacts (50 Å of Ti followed by 500 Å of Au) were deposited by e-beam evaporation while the undesired parts of the flake were removed using oxygen/argon plasma etching. The remaining graphene was protected with PMMA.

The temperature of the samples was set from 1.9 K up to 190 K using a ^4He cryostat. All the measurements were performed using standard ac lock-in techniques and four probe measurements. We applied an excitation current of $I = 50$ nA which was obtained by applying 5 V with frequency below 15 Hz to a 100 MΩ series resistance. This current flowed from contact S to D (see inset in Fig. 1). Also, pre-amplifiers with a gain of $\simeq\ 100$ were used to measure simultaneously the voltage drop V_{1-3}, V_{1-2} and V_{3-4} between the contact pairs $1-3$, $1-2$ and $3-4$ (see inset of Fig. 1). A 10 MW resistive magnet was used to apply a magnetic field up to 22 T perpendicularly to the TLG.

3 QHE in bilayer and trilayer graphene For the bilayer sample, we define the longitudinal resistance as $R_{xx} = (V_{1-2}/I)$ and the Hall resistance is defined as: $R_{xy} = (V_{1-3}/I)$. The Dirac point of this sample is at 25 V (see Fig. 2). We have characterized the bilayer sample by fitting the slope of the linear part of Hall resistances measured at different gate voltages. With this procedure we have obtained the carrier density at different gate voltages and we have used the value of the resistance at no magnetic field to calculate the mobility. The gate voltage varied from -40 V up to 14 V, the values of both the mobility and the density at the different gate voltages are:

V_{gate}(V)	$n_{2D}(10^{12}cm^{-2})$	$\mu(cm^2/Vs)$
-40	4.5	3800
-20	3.2	3600
-10	2.4	3557
0	1.6	3400
10	0.9	3127
14	0.7	2800

In Fig. 3 we show the QHE observed in a bilayer sample. This QHE differs from the QHE observed previously in monolayer graphene and reveals a new series of plateaus $\nu = \pm4, \pm8, \pm12, \pm16, ...$ not observed in monolayer graphene.

For the trilayer sample, we obtain the Hall resistivity using $\rho_{xy} = V_{1-3}/I$, and the longitudinal resistivity is obtained using $\rho_{xx} = (V_{1-2}/L)\,/\,(I/W)$. In Fig. 5 we show the Hall and longitudinal resistivities as a function of the magnetic field.

We obtain the mobility μ and 2D carrier density from the Hall and the longitudinal resistances at low magnetic field. The carrier density increases with increasing temperature, as expected for the semi-metallic TLG [9]. Unfortunately, we were not able to change the carrier concentration using the back gate voltage since there was a leak in the dielectric. Nevertheless, it has been shown that the carrier concentration can be changed using the back gate voltage [13].

We can see in Fig. 4 Hall resistivity shows the QHE with the presence of the $\nu = \pm6$ plateau. From the slope

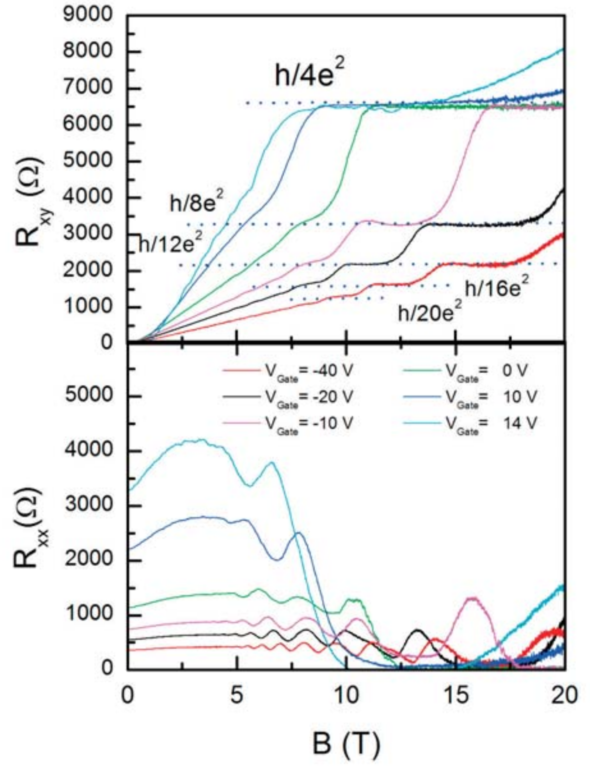

Figure 3 Measurements of the quantum Hall effect performed in a bilayer graphene flake at 2 K using the magnetic field as driving parameter at different gate voltages, varying from -40 V up to 14 V. The filling factor series for bilayer graphene $\nu = 4, 8, 12, 16, 20, \ldots$ is observed.

of the Hall resistivity we obtain the value of the carrier density $n_{2D} = 2.04 \times 10^{12}$ cm^{-2} and from the longitudinal resistance at 0 magnetic field we estimate a mobility of $\mu = 3750$ cm^2/Vs. For the density $n = 2.04 \times 10^{12} cm^{-2}$ of our sample at 4.5 K we calculate a filling factor $\nu = 6$ at a magnetic field of $B = nh/e\nu \sim 14$ T.

Once this analysis is performed, we calculate the components of the conductivity tensor by means of the usual relations

$$\sigma_{xx} = \frac{\rho_{xx}}{\rho_{xx}^2 + \rho_{xy}^2} \tag{1a}$$

$$\sigma_{xy} = \frac{\rho_{xy}}{\rho_{xx}^2 + \rho_{xy}^2} \tag{1b}$$

In Fig. 6 the components of the conductivity tensor σ_{xx} and σ_{xy} (calculated by means of Eq. (1a) and (1b)) at temperatures from 2 K up to 190 K as a function of the magnetic field are displayed. Concerning σ_{xy}, we can see a plateau at $\sigma_{xy} = 6e^2/h$ corresponding to $\rho_{xy} =$

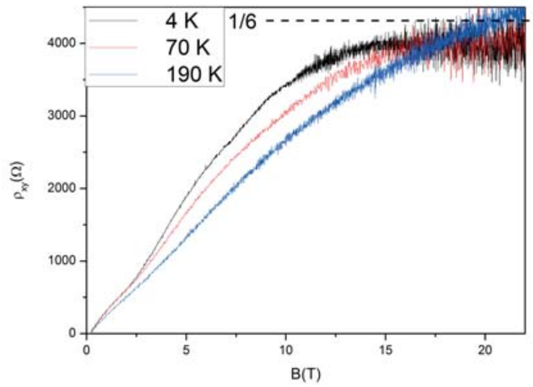

Figure 4 Hall (ρ_{xy}) resistivity versus B at temperatures 4.5, 70 and 190 K. The quantum Hall plateau at $\nu = \pm 6$ corresponding to $\rho_{xy} = h/6e^2$ is visible up to 70 K.

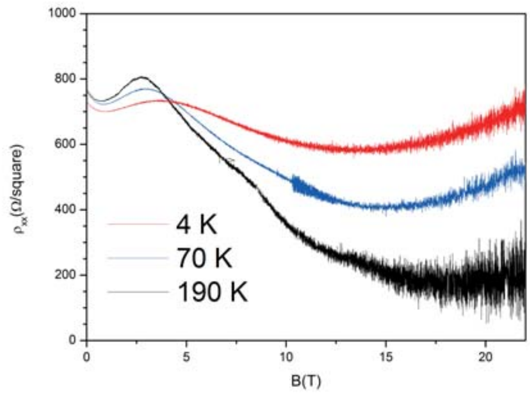

Figure 5 Longitudinal resistivities (ρ_{xx}) versus B at temperatures 4.5, 70 and 190 K.

$-h/6e^2 \sim -0.16h/e^2$. Some features observed at lower magnetic field suggest the presence of other unresolved quantum Hall plateaus. The Shubnikov-de Haas oscillations for our sample mobility are expected to begin for $B \sim 3$ T, so we can take this point as the beginning of the QHE regime. As mentioned above, the existence of a series of quantum Hall plateaus in TLG at filling factors $\nu = \pm 6, \pm 10, \pm 14, \ldots$ has been theoretically predicted [10]. Therefore, when the density is that which corresponds to the density at 4.5 K, we should expect the $\nu = 10$ QH plateau at $B \sim 7.7$ T and the $\nu = 14$ at $B \sim 5.5$ T. In Fig. 6 the Hall conductivity takes values close to $-10e^2/h$ for magnetic fields between 5 and 8 T.

4 Conclusions In conclusion, we have measured the quantum Hall effect in bilayer and trilayer graphene Hall

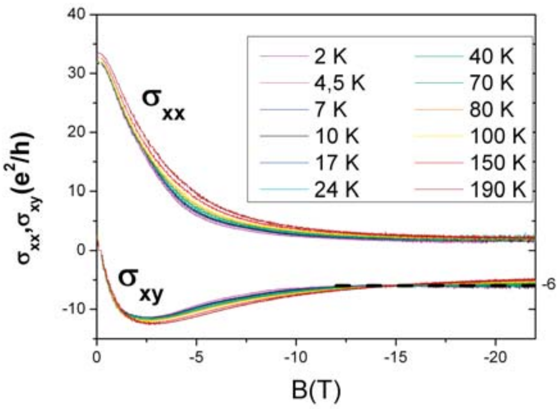

Figure 6 Hall conductivities of the trilayer graphene sample reported in fundamental units B at temperatures between 2 and 190 K. The quantum Hall plateau at $\nu = -6$ with $\sigma_{xy} = -6e^2/h$ is clearly evident at temperatures < 70 K.

bar observing the presence of the The resulting series of the quantum Hall plateaus for monolayer graphene is $\nu = \pm 4, \pm 8, \pm 12, \pm 16, 20, ...$ series for bilayer graphene and $\nu = \pm 6$ plateaus. We study the QHE dependance on the gate voltage for the bilayer device and the QHE dependance on temperature which is compatible with the expected features in the quantum Hall regime.

Acknowledgements This work was supported by the projects Cariplo Foundation QUANTDEV, MEC FIS2009-07880, PPT310000-2009-3, JCYL SA049A10-2, the FPU program by MEC and by EuroMagNET II under the EU contract no. 228043. The authors thanks J.M. Cerveró, G.P. Parravicini, L. Brey and F. Guinea for useful discussion.

References

[1] A. K. Geim and K. Novoselov, Nature Mater. **6**, 183 (2007).
[2] A. H. Castro Neto, F. Guinea, N. M. R. Peres, K. S. Novoselov, and A. K. Geim, Rev. Mod. Phys. **81**, 109 (2009).
[3] M. Vozmediano, M. Katsnelson, and F. Guinea, Phys. Rep. **496**, 109 (2010).
[4] A. Cresti, G. Grosso, and G. P. Parravicini, Phys. Rev. B **77**, 115408 (2008).
[5] N. M. R. Peres, Rev. Mod. Phys. **82**, 2673 (2010).
[6] K. S. Novoselov, A. K. Geim, S. V. Morozov, D. Jiang, M. I. Katsnelson, I. V. Grigorieva, S. V. Dubonos, and A. A. Firsov, Nature **438**, 197 (2005).
[7] Y. Zhang, Y.-W. Tan, H. L. Stormer, and P. Kim, Nature **438**, 201 (2005).
[8] K. S. Novoselov, E. McCann, S. V. Morozov, V. I. Falko, M. I. Katsnelson, U. Zeitler, D. Jiang, F. Schedin, and A. K. Geim, Nature Phys. **2**, 177 (2006).
[9] M. F. Craciun, S. Russo, M. Yamamoto, J. B. Oostinga, A. F. Morpurgo, and S. Tarucha, Nature Nanotechnol. **4**, 383 (2009).
[10] W. Zhu, V. Perebeinos, M. Freitag, and P. Avouris, Phys. Rev. B **80**, 235402 (2009).
[11] Y. Liu, S. Goolaup, C. Murapaka, W. S. Lew, and S. K. Wong, Effect of Magnetic Field on the Electronic Transport in Trilayer Graphene, Vol. 4 (2010), pp. 7087-7092, http://pubs.acs.org/doi/pdf/10.1021/nn101296x.
[12] W. Bao, Z. Zhao, H. Zhang, G. Liu, P. Kratz, L. Jing, J. Velasco, D. Smirnov, and C. N. Lau, Phys. Rev. Lett. **105**, 246601 (2010).
[13] A. Kumar, W. Escoffier, J. M. Poumirol, C. Faugeras, D. P. Arovas, M. M. Fogler, F. Guinea, S. Roche, M. Goiran, and B. Raquet, ArXiv e-prints (2011), arXiv:1104.1020 [cond-mat.mes-hall].
[14] E. Peled, Y. Chen, E. Diez, D. C. Tsui, D. Shahar, D. L. Sivco, and A. Y. Cho, Phys. Rev. B **69**, 241305 (2004).
[15] D.-K. Ki and H.-J. Le, Phys. Rev. B **79**, 195327 (2009).
[16] D.-K. Ki, S. Jo, and H.-J. Lee, Appl. Phys. Lett. **94**, 162113 (2009).
[17] C. H. Lui, Z. Li, Z. Chen, P. V. Klimov, L. E. Brus, and T. F. Heinz, Nano Lett. **11**, 164 (2011); http://pubs.acs.org/doi/pdf/10.1021/nl1032827.

